

Engineering
Electrical Engineering fields

Okayama University

Year 1996

Analysis and design of a DC
voltage-controlled static VAR
compensator using quad-series
voltage-source inverters

Hideaki Fujita
Okayama University

Shinji Tominaga
Okayama University

Hirofumi Akagi
Okayama University

This paper is posted at eScholarship@OUDIR : Okayama University Digital Information Repository.

http://escholarship.lib.okayama-u.ac.jp/electrical_engineering/7

Analysis and Design of an Advanced Static Var Compensator Using Quad-Series Voltage-Source Inverters

Hideaki Fujita, *Member, IEEE*, Shinji Tominaga, and Hirofumi Akagi, *Senior Member, IEEE*
Okayama University
Okayama 700, JAPAN

Abstract—This paper presents an advanced static var compensator (ASVC) using quad-series voltage-source inverters. The ASVC consists of four three-phase voltage-source inverters having a common dc capacitor and four three-phase transformers, the primary windings of which are connected in series to each other. Although each inverter outputs a square wave voltage, the synthesized output voltage of the ASVC has a 24-step wave shape. This results not only in a great reduction of harmonic currents and dc voltage ripples but also in less switching and snubbing losses.

This paper develops the analysis of the transient response and the resonance between ac reactors and the dc capacitor with the focus on practical use. Experimental results obtained from a small-rated laboratory model of 10kVA are also shown to verify the analysis leading to the design of the dc capacitor. The experimental and analytical results agree well each other.

I. INTRODUCTION

ATTENTION has been paid to advanced static var compensators (ASVCs) of 50 ~ 300MVA consisting of voltage-source inverters using GTO thyristors not only for improving power factor but also for stabilizing transmission systems. The ASVCs can adjust the amplitude of output voltage of the inverters by means of PWM or non-PWM operation, thus producing either leading or lagging reactive power [1]–[8].

A pulse-width-modulated ASVC [1]–[5], in which the dc voltage is controlled to remain a constant value, can achieve a high speed response of reactive power at the expense of increasing switching and snubbing losses. In practical applications of large capacity ASVCs to power systems, high efficiency is the first priority as well as high reliability be.

On the other hand, a dc voltage-controlled ASVC [6]–[8], which directly controls the dc capacitor voltage by adjusting a small amount of active power to flow into or out of the voltage-source inverters, results in less switching and snubbing losses because of non-PWM operation. However, it has been pointed out that the dc voltage-controlled ASVC is inferior in the transient response of reactive power to the pulse-width-modulated ASVC because of non-PWM operation. Some papers and articles dealing with the dc voltage-controlled ASVC have been published, but they have excluded the transient response of reactive power and the capacity or capacitance of the dc capacitor from analysis. Therefore, they have provided the following interpretations:

- The smaller the capacitance, the faster the response of reactive power.
- The larger the capacitance, the smaller the voltage

fluctuation across the dc capacitor.

In this paper, the analysis of the dc voltage-controlled ASVC consisting of quad-series voltage-source non-PWM inverters is presented, putting emphasis on the transient response of reactive power, and on the capacity of the dc capacitor. A new model for the ASVC based on the pq theory [1] is developed, which has the ability to deal with the power flow between the ac and dc sides in a transient state. The analysis leads to the following interesting phenomena which can not be explained by the conventional interpretations mentioned above:

- The capacity of the dc capacitor has almost no effect on the transient response of reactive power.
- The dc voltage fluctuation is not in inverse proportion to the capacitance.
- The ASVC falls into resonance between the dc capacitor and the ac reactors at a specified frequency.

Some experimental results obtained from a small-rated laboratory model of 10kVA agree well with the analytical results, verifying the validity of the interesting phenomena found out in the paper.

Moreover, it is shown by experiment and analysis that a feedback control loop of instantaneous reactive power makes it possible to achieve a fast response time of reactive power of 5msec.

II. VOLTAGE-CONTROLLED ASVC

A. Experimental System Configuration

Fig.1 shows a system configuration of an advanced static var compensator of 10kVA which consists of quad-series voltage-source inverters. The circuit parameters are shown in Table I. Each three-phase inverter is characterized by non-PWM operation, producing the output voltage of a six-step waveform. The dc links of the four voltage-source inverters are connected in parallel with a common dc capacitor of 500 μ F. The ac terminals of the inverters are connected to the supply via four three-phase transformers, the detailed configuration of which is shown in Fig.2. Each transformer has the three-phase windings of Δ or Y connection in the primary, which are separated phase by phase, and has the three-phase windings of Δ connection in the secondary. A voltage ratio of each transformer between the primary and secondary is 1:3.

In Fig.1, the inverters INV.1 and INV.3 operate at a leading phase-angle of 7.5° to the supply voltage, while INV.2 and INV.4 operate at a lagging one of 7.5°. This results in a great reduction of supply harmonic currents and dc link voltage ripples because the synthesized output

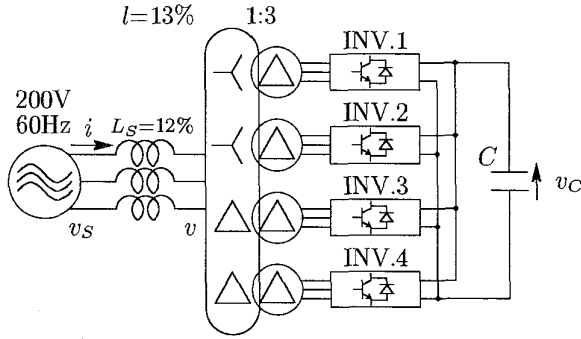


Fig. 1. Experimental system configuration.

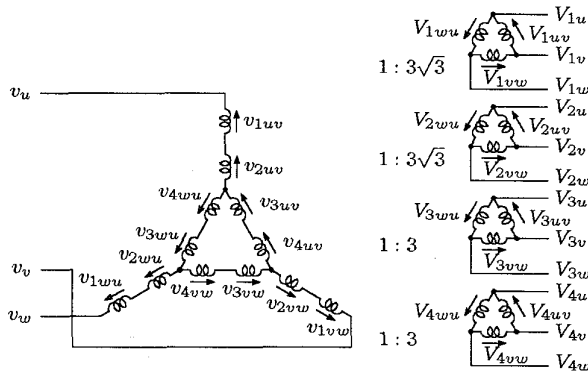


Fig. 2. Connection of four three-phase transformers.

voltage of the ASVC looks like a 24-step waveform. The fundamental component of the synthesized voltage is given by

$$V = \frac{\sqrt{6}}{\pi} \cdot \frac{m}{n} \cos \frac{\pi}{24} V_C, \quad (1)$$

where m is the number of the series connected inverters, and n means the voltage ratio of each transformer between the primary and secondary. Since $m = 4$ and $n = 3$ in the experimental system, the ratio of the fundamental voltage of the synthesized output to dc voltage of the ASVC, K is 1.03.

TABLE I

CIRCUIT PARAMETERS OF EXPERIMENTAL SYSTEM.

reactive power rating	Q	10kVA
line to line voltage of supply	V_S	200V
angular frequency of supply	ω_0	$2\pi \times 60\text{rad/s}$
dc voltage	V_C	150~250V
dc capacitance	C	500 μF
inductance of ac reactors	L_S	1.3mH(12%)
leakage inductance	l	1.4mH(13%)
equivalent resistance	R	0.28 Ω
ratio of dc voltage to ac voltage	K	1.03

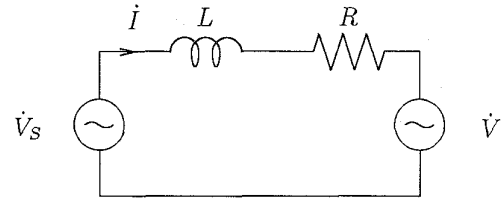


Fig. 3. Single phase equivalent circuit.

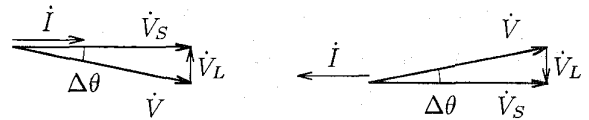


Fig. 4. Phasor diagram of ASVC.

B. Basic Principle in Steady State

Fig.3 shows a single-phase equivalent circuit of the ASVC. Here, \dot{V}_S is a supply voltage phaser, \dot{V} is an output voltage phaser of the ASVC, L and R are a reactor and a resistor included in the transformer. As well-known, the reactive power of the ASVC can be adjusted by controlling the amplitude of \dot{V} . If $|\dot{V}_S| > |\dot{V}|$, the ASVC produces a lagging reactive power, while, if $|\dot{V}_S| < |\dot{V}|$, it generates a leading one. The dc voltage-controlled ASVC can control the amplitude of the output voltage by adjusting a small amount of active power to flow into or out of the ASVC.

Fig.4(a) shows a phasor diagram in the case that \dot{V} lags to \dot{V}_S . Here, $\Delta\theta$ is a phase angle between \dot{V}_S and \dot{V} , and \dot{I} is a supply current phaser. In Fig.4(a), \dot{I} is in phase with \dot{V}_S , so that a small amount of active power flows into the ASVC, thus charging the dc capacitor. In the case that \dot{V} leads to \dot{V}_S , as shown in Fig.4(b), a small amount of active power flows out, thus discharging the dc capacitor. Accordingly, a large amount of reactive power produced by the ASVC can be controlled by adjusting a small amount of phase angle $\Delta\theta$.

III. TRANSIENT ANALYSIS FOR ASVC

A. Modeling for Transient Analysis of ASVC

For the sake of simplicity, the following assumptions are made in modeling of the ASVC:

1. Any harmonic voltage caused by the switching operation of the inverters is excluded from the synthesized output voltage of the ASVC.
2. The instantaneous amplitude of the synthesized output voltage is in proportion to the instantaneous voltage of the dc capacitor.
3. The active power on the ac side is equal to that on the dc side: No power loss occurs in the inverters.

Assumptions 1 and 2 mean that the harmonic voltage caused by fluctuation of the dc voltage is included in the synthesized output voltage, which has been excluded from

conventional modeling.

Assume an ideal three-phase power supply given by

$$\begin{bmatrix} v_{Su} \\ v_{Sv} \\ v_{Sw} \end{bmatrix} = \sqrt{\frac{2}{3}} V_S \begin{bmatrix} \cos \omega_0 t \\ \cos(\omega_0 t - 2\pi/3) \\ \cos(\omega_0 t + 2\pi/3) \end{bmatrix}, \quad (2)$$

where V_S is the rms voltage of the supply and ω_0 is its angular frequency. Assumptions 1 and 2 lead to the following output voltage of the ASVC.

$$\begin{bmatrix} v_u \\ v_v \\ v_w \end{bmatrix} = \sqrt{\frac{2}{3}} K v_C \begin{bmatrix} \cos(\omega_0 t + \Delta\theta) \\ \cos(\omega_0 t - 2\pi/3 + \Delta\theta) \\ \cos(\omega_0 t + 2\pi/3 + \Delta\theta) \end{bmatrix} \quad (3)$$

where $\Delta\theta$ is the angle between the supply and synthesized output voltage, and K is the ratio of the ac voltage to the dc voltage of the ASVC. Fig.3 gives the following equation.

$$\begin{bmatrix} v_{Su} \\ v_{Sv} \\ v_{Sw} \end{bmatrix} = \left(R + L \frac{d}{dt} \right) \begin{bmatrix} i_u \\ i_v \\ i_w \end{bmatrix} + \begin{bmatrix} v_u \\ v_v \\ v_w \end{bmatrix} \quad (4)$$

Assumption 3 means that the active power on the ac side equals that on the dc side of the ASVC as

$$p = v_u i_u + v_v i_v + v_w i_w = \frac{d}{dt} \frac{C}{2} v_C^2 = C v_C \frac{dv_C}{dt}. \quad (5)$$

The pq theory [1] makes a great contribution to transforming (2) ~ (5) to

$$\begin{bmatrix} L \frac{d}{dt} + R & -\omega_0 L \\ \omega_0 L & L \frac{d}{dt} + R \end{bmatrix} \begin{bmatrix} i_p \\ i_q \end{bmatrix} = \begin{bmatrix} V_S - K v_C \cos \Delta\theta \\ -K v_C \sin \Delta\theta \end{bmatrix}. \quad (6)$$

Eq.(5) is represented by using i_p and i_q as follows.

$$\frac{dv_C}{dt} = \frac{K}{C} (i_p \cos \Delta\theta + i_q \sin \Delta\theta) \quad (7)$$

In (6) and (7), i_p is an active power component and i_q is a reactive power component. The instantaneous reactive power drawn from the supply, q_S is given by

$$q_S = v_{Sp} \cdot i_q - v_{Sq} \cdot i_p = V_S \cdot i_q. \quad (8)$$

B. Transient Response of Reactive Power

Let's discuss the transient response of instantaneous reactive power q_S for a step change of phase angle $\Delta\theta$. However, non-linear functions, that is, the terms of $\sin \Delta\theta$ and $\cos \Delta\theta$, included in (6) and (7), make it difficult to directly solve the transient response of q_S . Assume that $\Delta\theta$ changes from 0 to $\Delta\theta_1$ as $\Delta\theta(t) = \Delta\theta_1 \cdot u(t)$, where $u(t)$ is a unit step function. the Laplace function for the reactive power $I_q(s)$ is obtained from (6) and (7), as

$$I_q(s) = -\frac{V_S \left\{ \frac{A_1}{L} s^2 + \left(\frac{R A_1}{L^2} + \frac{\omega_0 A_2}{L} \right) s + \frac{K^2 A_3}{L^2 C} \right\}}{s^3 + 2 \frac{R}{L} s^2 + \left(\frac{R^2}{L^2} + \frac{K^2}{LC} + \omega_0^2 \right) s + \frac{K^2 R}{L^2 C}} \quad (9)$$

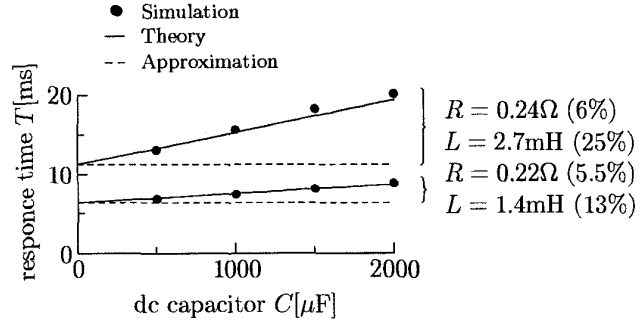


Fig. 5. Relationships between dc capacitance and time constant of response of q_S .

where

$$A_1 = \mathcal{L} [\sin \Delta\theta(t)] = (\sin \Delta\theta_1)/s$$

$$A_2 = \mathcal{L} [1 - \cos \Delta\theta(t)] = (1 - \cos \Delta\theta_1)/s$$

$$A_3 = \mathcal{L} [\sin \Delta\theta(t) \cos \Delta\theta(t)] = (\sin \Delta\theta_1 \cos \Delta\theta_1)/s$$

Assumption that $R^2/L^2 + K^2/LC \gg \omega_0^2$ produces the following approximate equation.

$$I_q(s) \approx \left(-\frac{B_1}{s} + \frac{B_1 - B_2}{s + R/L} + \frac{B_2 + B_3}{s^2 + (R/L)s + K^2/LC} \right) V_S \quad (10)$$

where

$$B_1 = (\sin \Delta\theta_1 \cos \Delta\theta_1)/R$$

$$B_2 = (1 - \cos \Delta\theta_1) \omega_0 C / K^2$$

$$B_3 = \sin \Delta\theta_1 (1 - \cos \Delta\theta_1) / L$$

The first and second terms on the right side in (10) are a dominant response of reactive power, while the third term means that an oscillatory component exists. The time constant of the transient response of reactive power, T is equal to the time constant determined by L and R in Fig.3.

$$T = \frac{L}{R}. \quad (11)$$

Note that the capacity or capacitance of the dc capacitor, C is excluded from (11). This means that an amount of the active power flowing into the ASVC is proportional to C at the time of the step change of $\Delta\theta$.

Fig.5 shows the relationship between the capacity of the dc capacitor and the time constant of the reactive power. The plots for $L(=l) = 1.4\text{mH}$ (13%) are also shown in Fig.5 because total inductance on the ac side, $L(=L_S + l) = 2.7\text{mH}$ (25%), which is used in the following experiments, may be larger than that in a practical system. The resistor R includes an equivalent resistance which is calculated from the losses of the transformers and the inverters because the losses are too large to be neglected. The solid lines indicate theoretical results without any approximation (see Appendix I), the broken lines show (10), and the dots show simulated results to verify the theory and approximation.

The simulated results concur with the theoretical lines. The theoretical lines show a small increase according to the capacity of the dc capacitor C . However, the difference between the theory and approximation is not so large in range of $C < 1000\mu\text{F}$ in which the capacitance of the dc capacitor used in the experiments exists. The approximation is applicable for usual practical systems having the reactors around 15% because the difference becomes small as the inductance of the ac reactors becomes small.

C. Resonance Between AC Reactors and DC Capacitor

As mentioned above, the third term in (10) is an oscillatory component. In other words, the dc voltage-controlled ASVC may fall into resonance between the ac reactors and the dc capacitor at a specific frequency. If a harmonic voltage, the frequency of which coincides with such a resonant frequency, were included in the supply, a large amount of harmonic currents would flow into the ASVC, and an excessive voltage fluctuation would then occur in the dc capacitor.

Assuming the resistance of $R = 0$ in (9), the resonant angular frequency is given by

$$\omega_R = \pm \sqrt{\frac{K^2}{LC} + \omega_0^2}. \quad (12)$$

Since ω_R is the angular frequency on the pq coordinates or on the dc side of the ASVC, the resonance occurs at $\omega_0 \pm \omega_R$ on the ac side of the ASVC.

To calculate the fluctuations of the dc voltage and the active power caused by the harmonic voltage in the supply, (6) is expanded as

$$\begin{bmatrix} R + L \frac{d}{dt} & -\omega_0 L \\ \omega_0 L & R + L \frac{d}{dt} \end{bmatrix} \begin{bmatrix} i_p \\ i_q \end{bmatrix} = \begin{bmatrix} v_{Sp} - K v_C \cos \Delta\theta \\ v_{Sq} - K v_C \sin \Delta\theta \end{bmatrix}, \quad (13)$$

where v_{Sp} and v_{Sq} are p and q components in the supply voltage, respectively.

Considering $\Delta\theta$ a constant value in (7) and (13), the Laplace transformed active power component $I_p(s)$ and dc voltage $V_C(s)$ are given as the following equations.

$$\begin{aligned} I_p(s) = & \frac{1/L}{s^3 + \frac{2R}{L}s^2 + \left(\frac{R^2}{L^2} + \frac{K^2}{LC} + \omega_0^2\right)s + \frac{K^2 R}{L^2 C}} \\ & \cdot \left\{ \left(s^2 + \frac{R}{L}s + \frac{K^2 \sin^2 \Delta\theta}{LC} \right) V_{Sp}(s) \right. \\ & \left. + \left(\omega_0 s^2 + \frac{K^2 \sin \Delta\theta \cos \Delta\theta}{LC} \right) V_{Sq}(s) \right\} \end{aligned} \quad (14)$$

$$\begin{aligned} V_C(s) = & \frac{K/LC}{s^3 + \frac{2R}{L}s^2 + \left(\frac{R^2}{L^2} + \frac{K^2}{LC} + \omega_0^2\right)s + \frac{K^2 R}{L^2 C}} \\ & \cdot \left[\left\{ \left(s + \frac{R}{L} \right) \cos \Delta\theta - \omega_0 \sin \Delta\theta \right\} V_{Sp}(s) \right. \\ & \left. + \left\{ \left(s + \frac{R}{L} \right) \sin \Delta\theta + \omega_0 \cos \Delta\theta \right\} V_{Sq}(s) \right] \end{aligned} \quad (15)$$

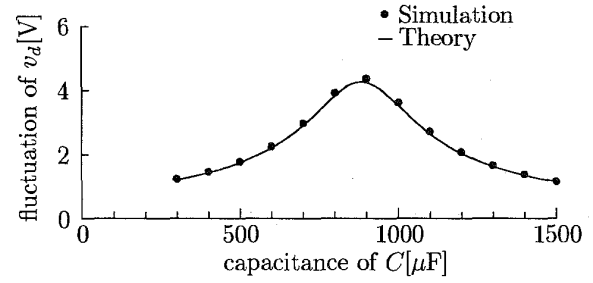


Fig. 6. Voltage fluctuation of dc capacitor caused by 3rd harmonic voltage of 1% in supply.

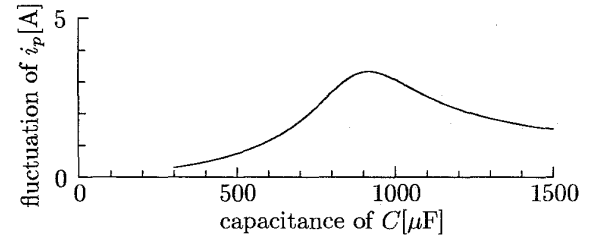


Fig. 7. Harmonic amplitude of i_p caused by 3rd harmonic voltage of 1% in supply.

Eq.(15) tells us that the amount of the dc voltage fluctuation is determined not only by the amplitude of the harmonic voltage included in the supply but also by the operating angle $\Delta\theta$.

Figs.6 and 7 show the dc voltage fluctuation V_C and the active power component I_p caused by a 3rd-order harmonic voltage of 1% which is included in the supply. Here, $\Delta\theta$ is a constant value of -0.06rad . The 3rd harmonics on the ac side of the ASVC make the dc voltage fluctuate at twice the supply frequency. In Fig.6, the maximum voltage fluctuation, which is 4V (2% of the dc voltage), appears at the point of $C = 900\mu\text{F}$ because the resonant frequency ω_R is equal to twice the supply frequency. At the point of resonance, the amplitude of the harmonic current in I_p reaches 3.5A, which is 10% of the rated current of the ASVC. The resonance would be a serious problem in a practical system, because an equivalent resistance in a practical system, R may be smaller than that of the experimental system.

The above analytical results don't agree with predictions in a conventional interpretation. The reason is a conflict between the following assumption of dc voltage fluctuation and the following calculation of the harmonic current in the conventional interpretation. That is, the harmonic current in the supply has been calculated under such an assumption that no harmonic voltage is included in the synthesized output of the ASVC. This means that any dc voltage fluctuation has been neglected. But the calculation of the dc voltage fluctuation has been performed based on the harmonic current calculated under the above assumption.

The dc voltage fluctuation affects the supply current in the new modeling developed in this paper because the output voltage of the ASVC includes the harmonic voltage caused by the dc voltage fluctuation. The resonance be-

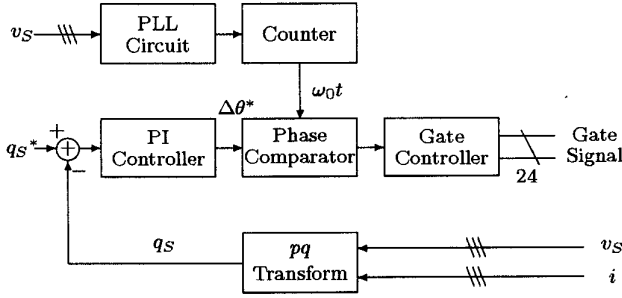


Fig. 8. Block diagram of control circuit.

tween the ac reactors and the dc capacitor occurs, when the harmonic voltage in the output increases the fluctuation of active power flowing into the ASVC. The dc voltage fluctuation becomes large as the capacitance increases up to $900\mu\text{F}$ as shown in Fig.6, when the harmonic voltage of the output cancels that in the supply and reduces the fluctuation of active power as shown in Fig.7.

IV. CONTROL CIRCUIT

Fig.8 shows the block diagram of the control circuit. The reactive power feedback using a PI controller makes it possible to improve the transient response of the reactive power. The pq transform circuit calculates the instantaneous reactive power q_s from the three-phase supply voltages v_{su} , v_{sv} , and v_{sw} and the three-phase currents i_u , i_v , and i_w . The calculated reactive power q_s , and the reference of reactive power, q_s^* are input to the PI controller which outputs a reference signal of phase angle $\Delta\theta^*$.

The counter produces the phase information, $\omega_0 t$, from a signal generated by the PLL circuit, the frequency of which is $49152(24 \times 2^{11})$ times of the supply. The phase comparator compares $\Delta\theta$ with $\omega_0 t$, and determines the time at which the corresponding switching device is turned on or off. The gate control circuit prevents each switching device from performing a multiple times of switching in one cycle caused by the fast change of $\Delta\theta$.

V. EXPERIMENTAL RESULTS

Figs.9 ~ 12 show simulated and experimental waveforms for a step change of $\Delta\theta$ from 0 to -0.08 rad under the same conditions except for the capacity of the dc capacitor. The output line-to-line voltage of the ASVC, v_{uv} has a 24-step wave shape, so that the supply current i_{su} is almost sinusoidal. Before $\Delta\theta$ is changed, i_{su} and q_s are equal to zero and the dc link voltage v_C is 190V. At the instance of the step change, v_C and q_s start rising up, and finally reach 230V and 10kvar in 50msec, respectively. The time constant of the transient response in Fig.10 is almost equal to that in Fig.12, which is 11msec, irrespective of the capacity of C . From (11), the theoretical time constant is given by

$$T = \frac{L}{R} = \frac{2.7\text{mH}}{0.24\Omega} = 11.2\text{msec},$$

which agrees well with the experimental result.

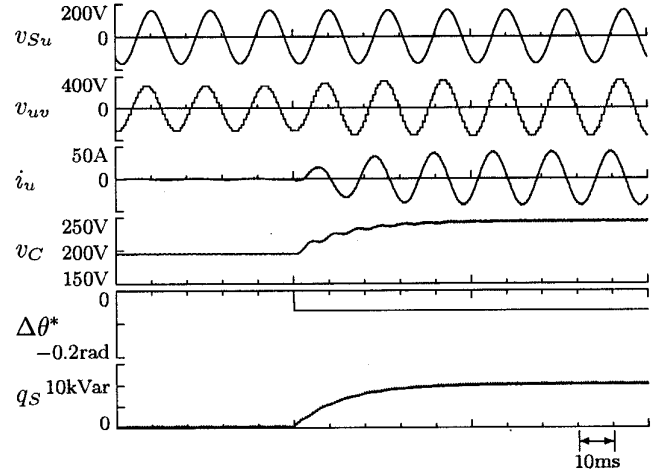


Fig. 9. Simulated waveforms for step change of $\Delta\theta$, where $C=500\mu\text{F}$.

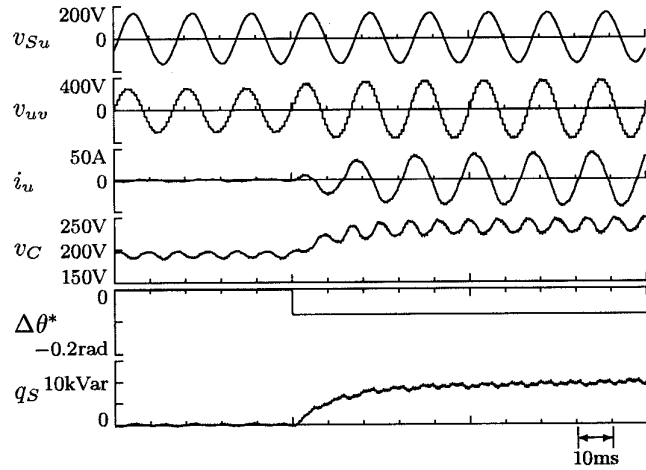


Fig. 10. Experimental waveforms for step change of $\Delta\theta$, where $C=500\mu\text{F}$.

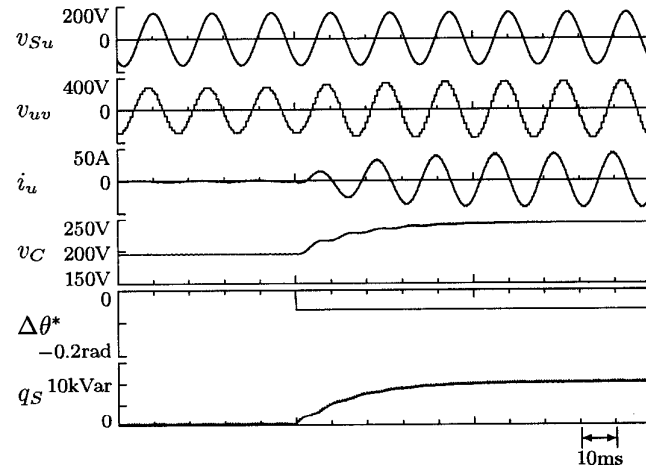


Fig. 11. Simulated waveforms for step change of $\Delta\theta$, where $C=1000\mu\text{F}$.

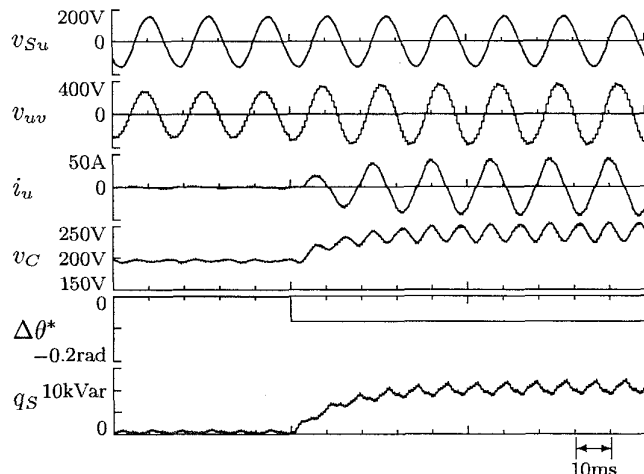


Fig. 12. Experimental waveforms for step change of $\Delta\theta^*$, where $C=1000\mu\text{F}$.

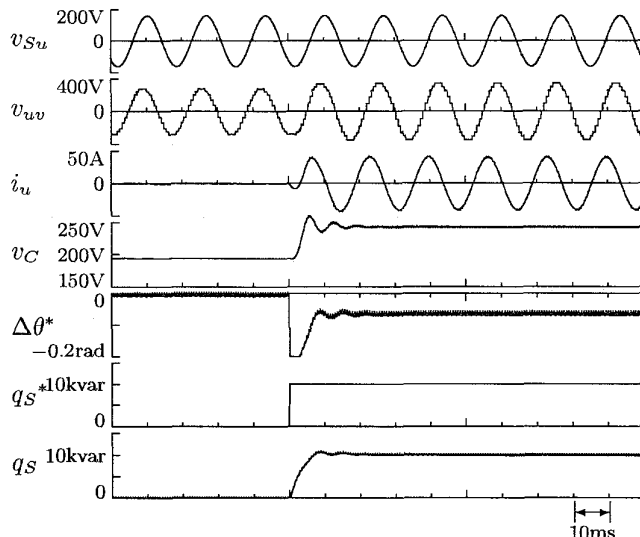


Fig. 13. Simulated waveforms for step change of q_S^* , where $C=500\mu\text{F}$.

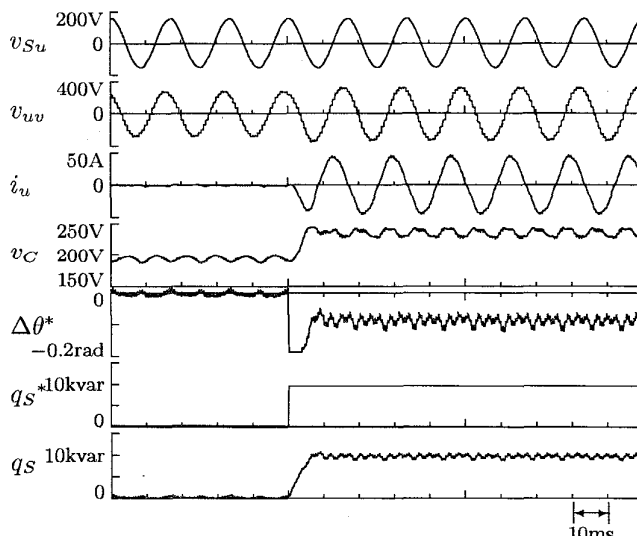


Fig. 14. Experimental waveforms for step change of q_S^* , where $C=500\mu\text{F}$.

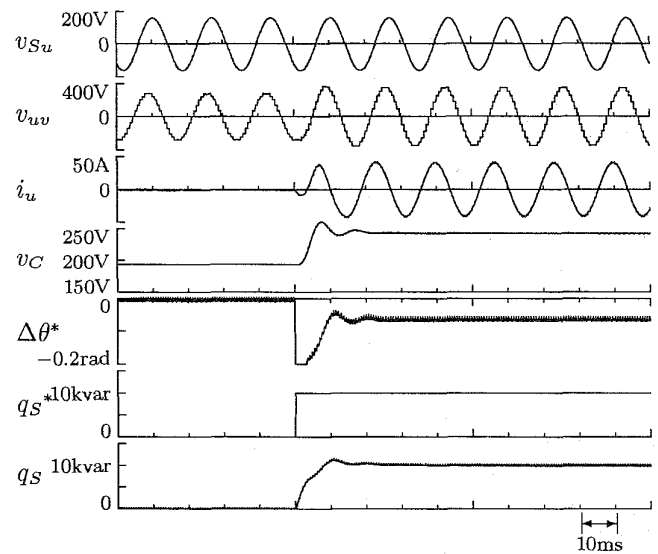


Fig. 15. Simulated waveforms for step change of q_S^* , where $C=1000\mu\text{F}$.

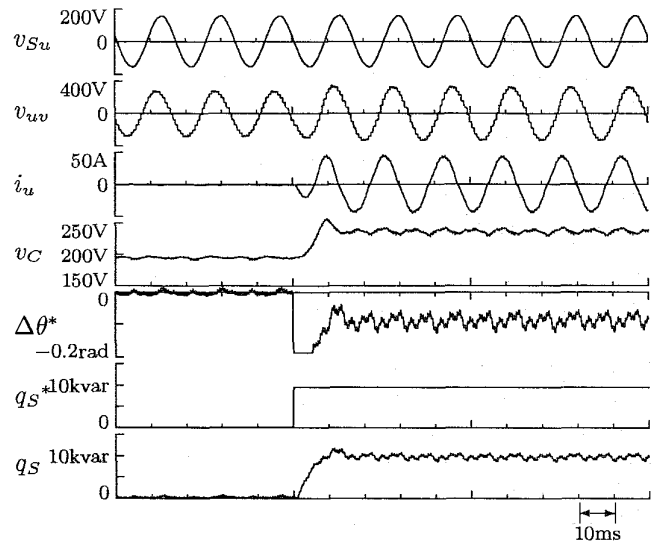


Fig. 16. Experimental waveforms for step change of q_S^* , where $C=1000\mu\text{F}$.

The voltage fluctuation of v_C in Fig.12 is larger than that in Fig.10, even if the capacity of C in Fig.12 is equal to twice of C in Fig.10. This is due to the resonance between the dc capacitor and the ac reactors, because the resonant frequency in Fig.12 is equal to twice the supply frequency of 60Hz. This shows that the reduction of the dc voltage fluctuation can be achieved, not by increasing the capacity of the dc capacitor, but by setting it to avoid the resonance.

Figs.13 ~ 16 shows experimental waveforms for a step change of the reactive power reference from 0 to 10kvar, where a reactive power feedback loop, having the feedback gain of $3.5 \times 10^{-5} \text{rad/var}$ and the time constant T_I of 11msec in a PI controller, is added to the control circuit. After the step change, v_C and q_S reached their final values in the steady state 10msec later. In Figs.14 and 16, the

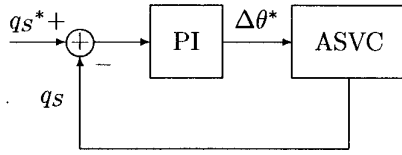


Fig. 17. Block diagram of ASVC without dc voltage-regulating control.

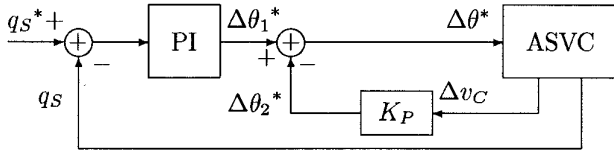


Fig. 18. Block diagram of ASVC with dc voltage-regulating control.

time constant of the transient response is 5msec, irrespective of the capacity of C , which is much faster than that required in the practical applications.

VI. EFFECT OF DC VOLTAGE-REGULATING CONTROL

The effect of dc voltage-regulating control is discussed in the following. Figs.17 and 18 show block diagrams of the ASVC, without (Fig.17) and with (Fig.18) the dc voltage-regulating control having only a proportional gain of K_p , respectively. Here, Δv_C is an amount of voltage variation. If $K_p = 0$, Fig.18 becomes the same as Fig.17.

Figs.19 and 20 show simulated results under the same parameters as Fig.13 except for adding the dc voltage control. A large fluctuation in the dc voltage appears in Figs.19 and 20 when compared with Fig.13. The dc voltage-regulating control has no effect on improving the stability of the dc voltage.

As well-known, addition of a current minor loop inside a speed major loop in an adjustable speed drive makes a great contribution to improving the stability of the torque control. The reason is that the response of the minor loop is much faster by 5 to 10 times than that of the major loop. However, the voltage-controlled ASVC has the same response time with respect to i_p , i_q and v_C because (9), (14) and (15) have the same characteristic equation. Thus, the dc voltage-regulating control does not act as a minor loop for improving the stability of the dc voltage.

VII. CONCLUSION

In this paper, the transient analysis of the dc voltage-controlled ASVC consisting of quad-series voltage-source non-PWM inverters has been explained in detail. A pq theory-based model for the ASVC has been developed to explore the transient behavior caused by power flow between the ac and dc sides. The experimental results obtained from the laboratory system show concurrence with the analytical ones.

The theoretical analysis explored in this paper has clarified the following interesting phenomena:

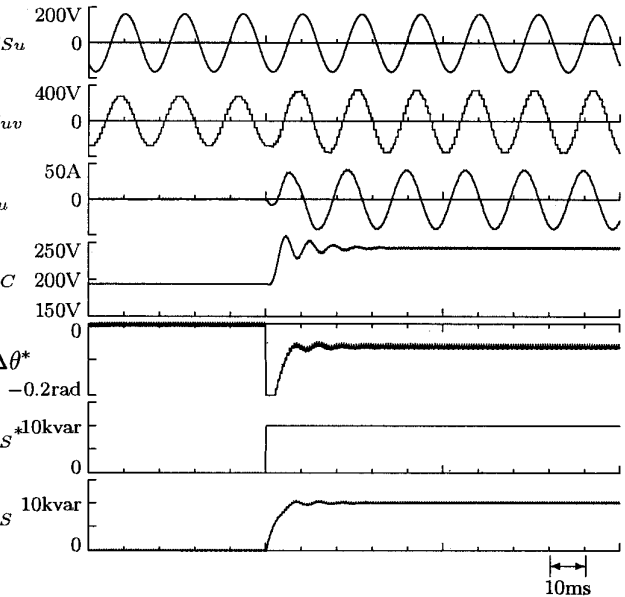


Fig. 19. Simulated waveforms in case of adding dc voltage control, where $K_p = -0.6 \times 10^{-3} \text{rad/V}$.

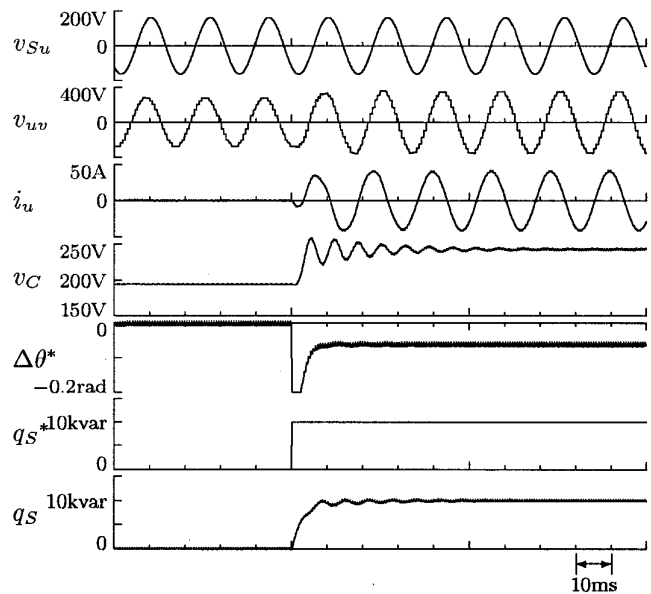


Fig. 20. Simulated waveforms in case of adding dc voltage control, where $K_p = -1.2 \times 10^{-3} \text{rad/V}$.

- The time constant of the transient response of reactive power is determined by the ac inductance and the equivalent resistance rather than the capacity of the dc capacitor.
- The ASVC may fall into resonance between the dc capacitor and the ac reactors at a specific frequency.

For the above reasons, the dc capacitor should be designed to avoid such resonance rather than to improve the transient response.

Moreover, the feedback control of instantaneous reactive power has made it possible to achieve a response time of 5msec, which is fast enough to be used in practical appli-

cations. The authors believe that the dc voltage-controlled ASVC is more suitable for compensating reactive power and/or stabilizing power systems than the pulse-width-modulated ASVC.

APPENDIX

I. TRANSIENT RESPONSE WITHOUT APPROXIMATION

The approximation in (10) can be applied to a usually designed system, but not to an ASVC which is equipped with a very large capacitor on the dc side. Assuming that $-\alpha$ is a real root of the characteristic equation, (9) can be represented by using α as

$$\begin{aligned} I_q(s) &= -\frac{1}{(s+\alpha)(s^2+\beta s+\gamma)} \left\{ \frac{\sin \Delta\theta}{L} s + \frac{R}{L^2} \sin \Delta\theta \right. \\ &\quad \left. + \frac{\omega_0}{L} (1 - \cos \Delta\theta) + \frac{K^2}{L^2 C s} \sin \Delta\theta \cos \Delta\theta \right\} \cdot V_S \\ &= \left(\frac{D_1}{s+\alpha} + \frac{D_2 s + D_3}{s^2 + \beta s + \gamma} \right) \cdot \frac{V_S}{s} \\ &= \left(\frac{D_1/\alpha + D_3/\gamma}{s} - \frac{D_1/\alpha}{s+\alpha} \right. \\ &\quad \left. - \frac{(s+\beta)D_3\gamma - D_2}{s^2 + \beta s + \gamma} \right) V_S \end{aligned} \quad (16)$$

where

$$\begin{aligned} D_1 &= \frac{1}{\alpha^2 - \alpha\beta + \gamma} \left\{ \frac{R\alpha}{L^2} \sin \Delta\theta + \frac{\omega_0\alpha}{L} (1 - \cos \Delta\theta) \right. \\ &\quad \left. - \frac{\alpha^2}{L} \sin \Delta\theta - \frac{K^2}{L^2 C} \sin \Delta\theta \cos \Delta\theta \right\} \\ D_2 &= -\frac{\sin \Delta\theta}{L} - D_1 \\ D_3 &= -\frac{R}{L^2} \sin \Delta\theta - \frac{\omega_0}{L} (1 - \cos \Delta\theta) + \frac{\alpha}{L} \sin \Delta\theta + \\ &\quad D_1(\alpha - \beta) \end{aligned}$$

Thus, the time constant of the response of reactive power is given by

$$T = \frac{1}{\alpha}. \quad (17)$$

Although the analytical solution of α is too complex, the numerical solution can be easily obtained by means of a numerical calculation using a computer.

REFERENCES

- [1] H. Akagi, Y. Kanazawa, and A. Nabae, "Instantaneous Reactive Power Compensators Comprising Switching Devices without Energy Storage Components," *IEEE Trans. on IAS*, vol. IA-20, no. 3, pp. 625-630, May/June, 1984.
- [2] L. T. Morán, P. D. Ziogas, and G. Joos, "Analysis and Design of a Three-Phase Synchronous Solid-State Var Compensator," *IEEE Trans. Ind. Applicat.*, vol. IA-25, no. 4, pp. 598-608, July/Aug. 1989.
- [3] F. Ichikawa, K. Suzuki, T. Nakajima, S. Irokawa, and T. Kitahara, "Development of Self-Commutated SVC for Power System," in *proc. 1993 PCC-Yokohama*, no. D1-6, pp. 609-614.
- [4] K. Suzuki, T. Nakajima, S. Ueda, Y. Eguchi, "Minimum Harmonic PWM Control for Self-Commutated SVC," in *proc. 1993 PCC-Yokohama*, no. D1-7, pp. 615-620.
- [5] N. S. Choi, G. C. Cho, and G. H. Cho, "Modeling and Analysis of a Static Var Compensator Using Multilevel Voltage Source Inverter," in *Proc. 1993 IAS Ann. Mtg. (Toronto)*, pp. 901-908.
- [6] L. Gyugyi, "Reactive Power Generation and Control by Thyristor Circuit," *IEEE Trans. Ind. Applicat.*, vol. IA-15, no. 5, pp. 521-532, Sept./Oct. 1979.
- [7] Y. Sumi, Y. Harumoto, T. Hasegawa, M. Yano, K. Ikeda, and T. Matura, "New Static Var Control Using Force-Commutated Inverters," *IEEE Trans. PAS*, vol. PAS-100, no. 9, pp. 4216-4223, Sept. 1981.
- [8] L. Gyugyi, N. G. Hingorani, P. R. Nannery, and N. Tai, "Advanced Static Var Compensator Using Gate Turn-off Thyristors for Utility Applications," *CIGRE*, 1990 Session, 23-203.